Phycologia (2007) Volume 46 (5), 572–582 Published 4 September 2007

Scrippsiella irregularis sp. nov. (Dinophyceae), a new dinoflagellate from the southeast coast of Iran

GILAN ATTARAN-FARIMAN* AND CHRISTOPHER J.S. BOLCH

School of Aquaculture, University of Tasmania, Locked Bag 1370, Launceston, Tasmania 7250, Australia

G. ATTARAN-FARIMAN AND C.J.S. BOLCH. 2007. *Scrippsiella irregularis* sp. nov. (Dinophyceae), a new dinoflagellate from the southeast coast of Iran. *Phycologia* 46: 572–582. DOI: 10.2216/07-02.1

A new species of *Scrippsiella* is described by light and electron microscopy from laboratory cultures established from resting cysts collected from the southeast coast of Iran. Comparative morphological analyses and sequencing of the rDNA-ITS and 5.8S rDNA show that the new species, *Scrippsiella irregularis* sp. nov., is allied to but distinct from *Scrippsiella precaria* and *S. ramonii*. Vegetative cells of the new species are similar in size, shape, and plate tabulation to *S. precaria*; however, the cingulum is equatorially placed, the nucleus is in the hypocone, and the second anterior intercalary plate is larger and rounded rather than diamond-shaped. The resting cysts isolated from sediments and produced in laboratory cultures are spherical to ovoid with numerous pointed to slightly capitate calcareous processes.

KEY WORDS: *Scrippsiella*, Resting cyst, DNA, Phylogeny, rDNA-ITS, Iran, Oman Sea

INTRODUCTION

Phytoplankton cells of the photosynthetic dinoflagellate genus *Scrippsiella* Balech & Loeblich III species are relatively small (15–40 μm) thecate, autotrophic cells that generally produce calcareous resting cysts. A few species produce organic-walled cysts, such as *Scrippsiella hangoei* Schiller (Larsen *et al.* 1995) and *Scrippsiella imariense* Kobayashi & Matsuoka (Kobayashi & Matsuoka 1995).

Phytoplankton cells and resting cysts of *Scrippsiella* species are regular and dominant components of the dinoflagellate flora of coastal marine waters and sediments around the globe (Honsell & Cabrini 1991; Faust 1996; Godhe *et al.* 2000; Montresor *et al.* 2003). In tropical and subtropical regions, the diversity and abundance of *Scrippsiella* resting cysts appears to be as high or higher than that of temperate regions (Dale 1992; Vink 2004), yet our knowledge of the diversity of the genus from the tropical phytoplankton is very limited.

During a study of dinoflagellate cysts from tropical southeast coast of Iran, we found several *Scrippsiella*-like calcareous cyst types that could be germinated to produce a range of morphologically distinct *Scrippsiella* cells. Some morphotypes established from these germinations exhibited asymmetrically arranged intercalary plates. In this paper we compare the cyst and cell morphology and nucleotide sequence of the rDNA-ITS and 5.8S-rDNA of these cells with those of related species and describe a new species, *Scrippsiella irregularis* sp. nov., from laboratory cultured material.

MATERIAL AND METHODS

Sediment collection and processing

Sediment samples were collected by an Ekman grab from three locations: the Bahoo-Kalat estuary, the coastal area near Pasabandar, and Chabahar Bay on the southeast coast of Iran (Fig. 1). The surface sediment from the grab samples was bottled and transported in the dark at 20°C until it was processed in the laboratory. Approximately 2–4 g of wet sediment were mixed with 0.2-μm filtered seawater in an 80-ml plastic container to obtain a watery slurry and sonicated for 2 min using a Microson ultrasonic cell disruptor (small probe, 200 W) to separate detrital particles from resting cysts. Samples were filtered through a 125-μm sieve, collected on a 20-μm sieve (Bolch & Hallegraeff 1990), and resuspended in distilled water. Live resting cysts were then concentrated using a two-step density gradient centrifugation consisting of an upper layer composed of distilled water (1.0 g cm^{-3}) and a lower layer of sodium polytungstate (1.3 g cm^{-3}) (Bolch 1997).

Cyst germination and culture experiments

Individual cysts were isolated from processed and washed sediment suspensions using a flame-drawn micropipette and a Leica stereomicroscope. Cysts were washed twice in sterile GSe growth medium (GSe medium, 35-ppt salinity; Blackburn *et al.* 1989), placed individually in 55-mm polystyrene Petri dishes containing 10 ml of GSe medium which were then sealed with Para-film and incubated at 27 ± 0.5°C under cool-white fluorescent light (70–90 μmol photons PAR $m^{-2} s^{-1}$) with a 12-h light : 12-h dark cycle. After germination, cells were allowed to divide and grow to a cell concentration sufficient for transfer to 100-ml Erlenmeyer flasks containing 50 ml of growth medium. Resultant clones were subcultured every 4 weeks. Separate subcultures were also acclimatised to lower temperatures by transfer to 23°C for at least one transfer cycle (3 weeks) followed by transfer to 17°C for long-term culture maintenance.

For encystment studies, *S. irregularis* strains SCBC17 and SCBC19 maintained at 27°C were each inoculated into polystyrene Petri dishes containing 20 ml of nitrate- and phosphate-deficient GSe medium and incubated under the conditions described above. Dishes were examined regular-

* Corresponding author (gilanattaran@ifro.ir).

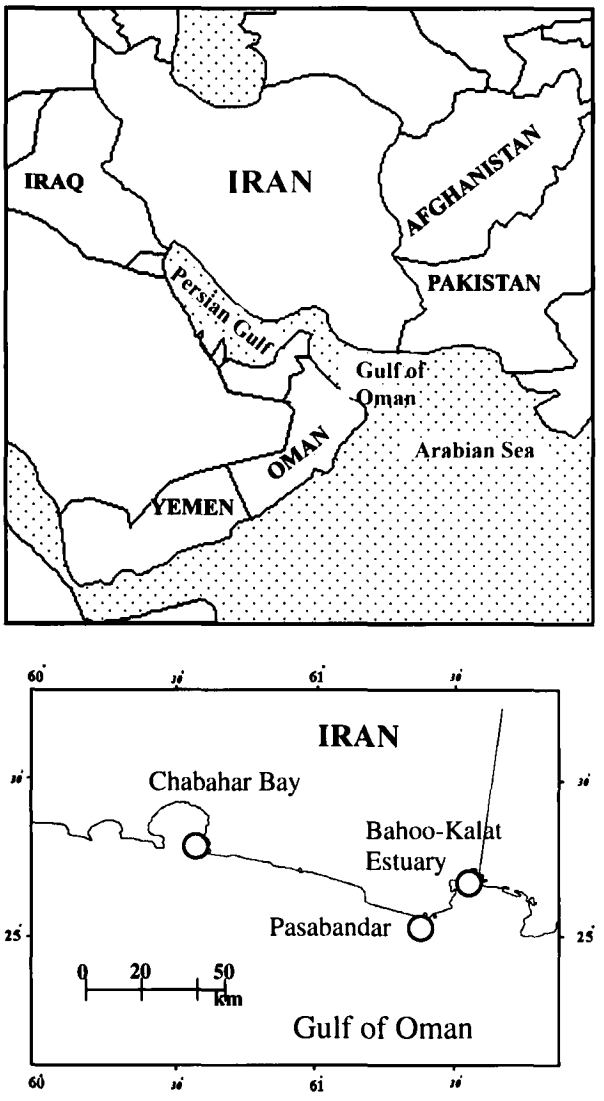

Fig. 1. Map of the study area showing sites from which triplicate surface sediment samples were collected.

ly for the presence of calcareous resting cysts, which were then examined using light and scanning electron microscopy (SEM).

Microscopy

Cultured and wild resting cysts of *S. irregularis* were photographed with an Olympus BH-2 light microscope equipped with a Leica DC300F digital imaging system. The plates of germinated thecate cells were stained with Calcofluor M2R (Fritz & Treimer 1985) and examined by fluorescent microscopy using a broadband UV filter (Olympus filter set no. 488). For SEM, cells in a 10-ml aliquot of culture were concentrated by centrifugation (5 min at 1000 × g), collected on poly-lysine–coated coverslips (Marchant & Thomas 1983) and dehydrated in a graded methanol series (10–100% in eight steps). Mounted specimens were then dried from hexamethyldisilazane (Nation 1983) and placed on SEM stubs for examination by SEM. Individual cysts were also isolated from processed sediments, washed twice in distilled water, placed on 1-μm Nucleopore filters, and air-dried before mounting the filters on SEM stubs. All stubs were sputter-coated with gold and examined with a Philips Quanta 600 or JEOL JSM-840 scanning electron microscope.

DNA extraction and sequencing

Approximately 10 ml of exponential growth-phase cultures SCBC17, SCBC19 were pelleted by gentle centrifugation (1500 × g for 5 min) and the supernatant discarded. DNA was extracted using a phenol/chloroform, gentle-lysis method described by Bolch *et al.* (1998). The extracted DNA was precipitated by the addition of one-tenth volume of 3 M sodium acetate and two volumes of cold ethanol, and the DNA pelleted recovered by centrifugation for 20 min at 14,000 × *g*. Cell pellets were washed twice in 70% ethanol, air-dried, and resuspended in sterile Milli-Q water or TE buffer. DNA quality was verified by 1% agarose gel electrophoresis, and subsamples were diluted to an approximate concentration of 10 ng μl^{-1} and used as templates for PCR. The internal transcribed spacer and 5.8S rRNA gene (rDNA-ITS) region was amplified using the primers ITSA [5′-CCA AGC TTC TAG ATC GTA ACA AGG (ACT) TCC GTA GGT-3′] and ITSB [5-CCT GCA GTC GAC A(TG) ATG CTT AA(AG) TTC AGC (AG)GG-3′] (Adachi *et al.* 1994).

PCR reactions were performed in 50-μl volumes in thin-walled 200-μl PCR tubes. The PCR reactions contained Bioline NH_4 PCR reaction buffer [160 mM $(NH_4)_2SO_4$, 670 mM Tris-HCL, and 0.1% Tween-20], 3 mM $MgCl_2$, 200 μM dNTPs, 10 pM of each primer, 1 U BioTaq DNA polymerase (Bioline, UK), and 10 ng of template DNA. Thermocycling was as follows: initial denaturation of 2 min at 94°C, followed by 35 cycles of 94°C for 1 min, annealing at 60°C for 1 min, elongation at 72°C for 2 min, and a final extension of 6 min at 72°C. The PCR products were stored at −20°C until further analysis. The presence of the specific amplification products were verified using agarose gel electrophoresis. Successful PCR products were purified using Montage™ PCR Devices (Millipore, Billerica, MA, USA) according to the manufacturer's protocols, and DNA was quantified using a Turner TBS-380 DNA fluorometer. Purified PCR products were sequenced in both directions with the forward or the reverse primer using a Dye Terminator Sequencing Kit (Beckman-Coulter, Fullerton, CA, USA) following the manufacturer's protocols and completed reactions electrophoresed on a Beckman-Coulter CEQ2000 capillary sequencer.

Alignment and phylogenetic analyses

Nucleotide sequences were checked by manual inspection of electropherograms in both directions and base-calling errors corrected manually using the software program BioEdit (Hall 1999). Sequences obtained from the present study and related dinoflagellate sequences available from GenBank were aligned using ClustalX version 1.83 (Jeanmougin *et al.* 1998) and improved by manual inspection. PAUP* 4.0b10 for Macintosh (Swofford 2002) was used for phylogenetic analyses. Initial neighbour-joining analyses included 56 rDNA-ITS sequences from Calciodinellaceaean dinoflagellates (Table 1) to establish

Table 1. Details of the 56 strains and GenBank accession numbers of DNA sequences used in preliminary analyses. The 27 DNA sequences used in the final phylogenetic analyses are indicated (+). Sequences generated during this study indicated in bold text.

Taxon	Strain no.	GenBank no.	Reduced data set
Calciodinellum albatrosianum	GeoB 149	AY676143	
Calciodinellum albatrosianum	M34-*26/4	AY676145	+
Calciodinellum albatrosianum	M34-17	AY676144	
Calciodinellum levantinum	GeoB 122	AY676146	+
Calciodinellum levantinum	GeoB*165	AY676147	
Calciodinellum operosum	CalopeD006	AY327462	+
Calciodinellum sp.	GeoB 120	AY676148	+
Ensiculifera aff. *imariensis*	D207	AY728076	+
Ensiculifera cf. *imariensis*	JB3	AF527814	+
Ensiculifera loeblichi	UTEXLB1595	AF527815	+
Heterocapsa pygmaea	CCMP1322	AB084093	+
Heterocapsa triquetra	NIES 7	AB084101	+
Pentapharsodinium dalei	SZN19	AF527817	+
Peridinium cinctum	CCAC 0102	AY499511	+
Pernambugia tuberosa	GeoB 61	AY499519	+
Scrippsiella hangoei	SHTV1	AY499515	+
Scrippsiella infula	GeoB 110	AY499523	+
Scrippsiella irregularis	**SCBC17**	**EF584460**	+
Scrippsiella irregularis	**SCBC19**	**EF584461**	+
Scrippsiella lachrymosa	D192	AY728078	+
Scrippsiella lachrymosa	IO 25-01	AY676150	
Scrippsiella precaria	CS-294	AY499518	+
Scrippsiella ramonii	SZN7	AF527820	+
Scrippsiella rotunda	SZN66	AF527821	+
Scrippsiella sp.	CS-168	AY499533	
Scrippsiella sp.	D1006	AY728079	
Scrippsiella sp.	GeoB 138	AY499525	
Scrippsiella sp.	GeoB 188	AY499524	
Scrippsiella sp.	GeoB*160	AY499526	
Scrippsiella sp.	GeoB*161	AY499527	
Scrippsiella sp.	M34-*25/5	AY499531	+
***Scrippsiella* sp.**	**SCBC21**	**EF584453**	
***Scrippsiella* sp.**	**SCBC116**	**EF584459**	
Scrippsiella sweeneyae	NIES 684	AY499520	+
Scrippsiella trifida	GeoB 109	AY499521	+
Scrippsiella trochoidea	D201	AY728080	
Scrippsiella trochoidea	GeoB*200	AY676157	
Scrippsiella trochoidea	GeoB*201	AY676158	
Scrippsiella trochoidea	GeoB*214	AY676160	
Scrippsiella trochoidea	IO 14-01	AY676162	
Scrippsiella trochoidea	IO 26-01	AY676163	
Scrippsiella trochoidea	NIES 369	AY499530	+
Scrippsiella trochoidea	SZN33	AF527070	
Scrippsiella trochoidea	SZN61	AF527075	
Scrippsiella trochoidea	SZN64	AF527079	
Scrippsiella trochoidea	SZN82 clone 49	AF527101	+
Scrippsiella trochoidea	**SCPC18**	**EF584454**	
Scrippsiella trochoidea	**SCPC36**	**EF584455**	
Scrippsiella trochoidea	**SCPC39**	**EF584458**	
Scrippsiella trochoidea	**SCPC51**	**EF584457**	
Scrippsiella trochoidea	**SCPC73**	**EF584456**	
Scrippsiella trochoidea var. *aciculifera*	GeoB 228	AY499529	+
Scrippsiella trochoidea var. *aciculifera*	GeoB*213	AY676164	
Scrippsiella trochoidea var. *aciculifera*	SCCAP499	AF527066	
Scrippsiella trochoidea var. *aciculifera*	SZN60	AF527071	
Scrippsiella trochoidea var. *aciculifera*	SZN63 clone 135	AF527078	+

the major branching patterns and clusters among the taxa. However, the analytical time required for maximum likelihood and parsimony analyses with this large data set was unworkable; therefore the data set was reduced to 27 taxa by excluding identical sequences and reducing each terminal cluster to one or two representatives. The final alignment contained 757 characters (including gaps introduced for alignment purposes). The peridinioid taxa *Heterocapsa pygmaea* A.R. Loeblich, *Heterocapsa triquetra* Ehrenberg (Stein), and *Peridinium cinctum* Muller were used as outgroups to root the analyses.

Significant phylogenetic structure in the data set was estimated by the random tree method and probability tables using the critical values of g_1 (Hillis & Huelsenbeck 1992). Phylogenetic trees were constructed using neighbour-joining (NJ) and maximum parsimony (MP). NJ analyses used the mean distance and logDet-Paralinear distance matrices. Most parsimonious trees were found using the branch and

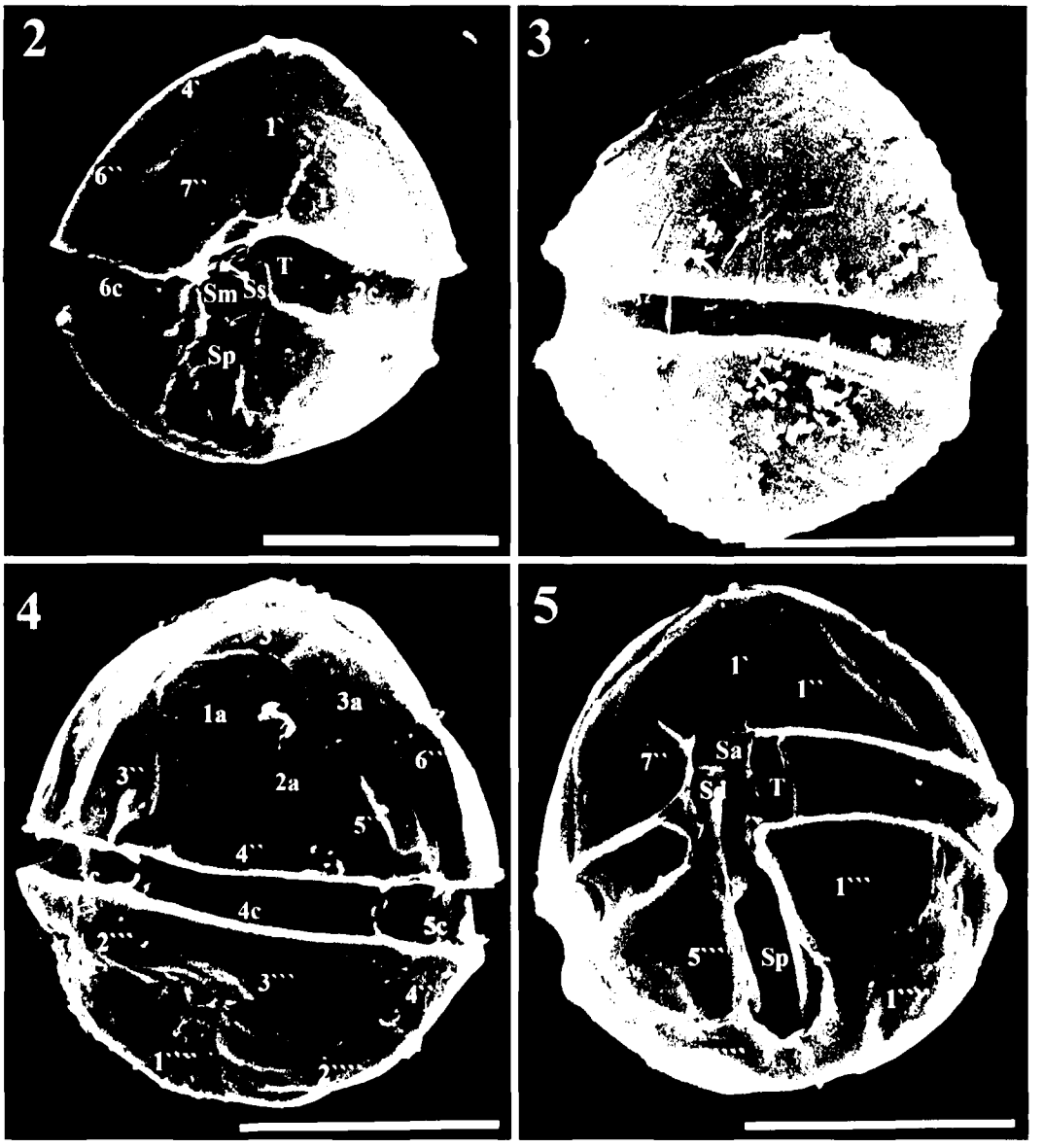

Figs 2–5. SEM. Vegetative cell of *Scrippsiella irregularis* (Fig. 2—1C19; Fig. 3—1C17; Figs 4, 5—2C19). All scale bars = 10 μm.
Fig. 2. Ventral view showing the plate pattern.
Fig. 3. Dorsal view showing the second intercalary plate (arrows) and slight narrowing of the cingulum on the dorsal side of the cell.
Fig. 4. Dorsal view of cell showing the plate pattern and rounded shape and size of 2a plate.
Fig. 5. Ventral view showing sulcal and postcingular (1‴, 5‴) plates. Note the S_m plate almost hidden by wing of S_d plate.

bound algorithm. All characters were equally weighted, and gaps were treated as missing data, with multistate characters (DNA ambiguities) interpreted as uncertainty. Bootstrap analyses of NJ and MP trees (Felsenstein 1985) utilised 200 replicates of the heuristic search algorithm.

RESULTS

Description and observations

***S. irregularis* Attaran-Fariman & Bolch sp. nov.**

Figs 2–19

Cellulae ovoideae, leviter dorsiventraliter compressae, 17–29 μm longae, 13–23 μm latae. Epitheca rotundata, conica lateribus convexis, sine cornu apicali; hypotheca rotundata. Cingulum subaequatoriale descendens, per dimidiam partem vel per totum latitudinis suae dislocatum. Formula laminarum Po, X, 4′ 3a, 7″, 6C (5C+1), 6S, 5‴, 2⁗. Laminae 1a et 3a adjacentes, hexagonae et forma similes. Lamina 2a infra et inter laminas 1a et 3a, subrectangularis vel rotundata. Sulcus valde distinctus, antapicem non attingens. Lamina anterior sulcalis (Sa) latior quam longior, super porum flagellarum et laminas sulcales extensa. Nucleus magnus sphaericus, in hypotheca. Chloroplasti aliquot, globulares, peripherales, fuscovirides. Cystae quiescentes sphaericae vel ovoideae, 20–26 μm in diametro, spinis multis calcareis acicularibus vel capitatis 3.5–4.5 μm longis.

Cells ovoid in outline, slightly dorsoventrally compressed, 17–29 μm long, 13–23 μm wide. Epitheca rounded, conical with convex sides and no apical horn; hypotheca rounded. Cingulum subequatorial and descending, displaced one-half to one

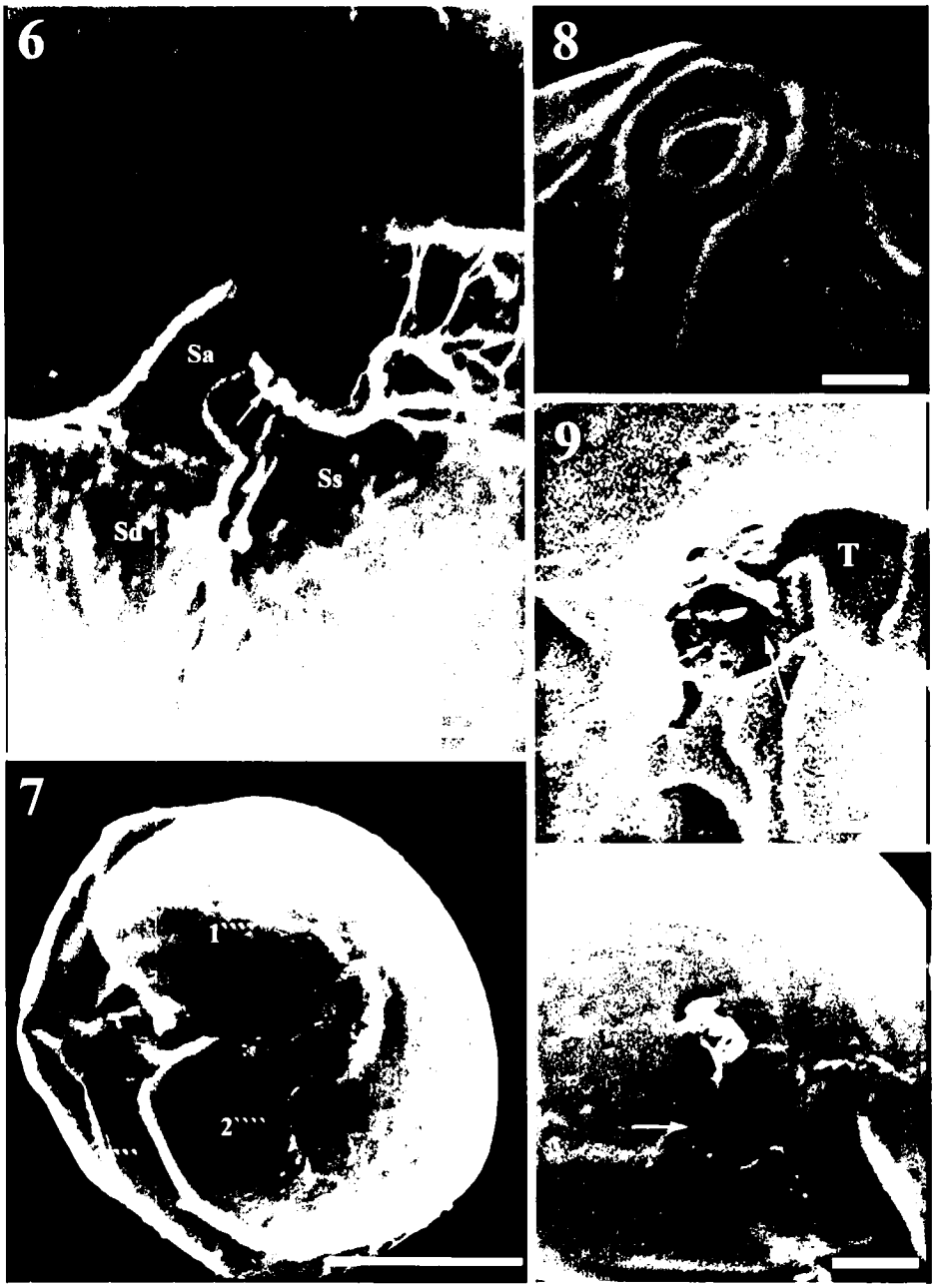

Figs 6-10. SEM. Vegetative cell of *Scrippsiella irregularis* (Fig. 6—1C17; Fig. 7—1C19; Fig. 8—2C17; Fig. 9—1C17; Fig. 10—2C19). All scale bars = 2 μm, except Fig. 6 = 10 μm.

Fig. 6. Sulcal area showing the transverse and longitudinal flagella. Note the shape of S_a and S_d plates.

Fig. 7. Antapical view of cell.

Fig. 8. Apical view showing apical pore and canal plates.

Fig. 9. Sulcal plates, showing the shape of S_m (left arrow) and S_s plates (right arrow) and the transitional plate.

Fig. 10. Dorsal view, showing intercalary plates, note 2a plate (arrow).

cingulum width, narrowing dorsally. Plate formula Po, X, 4′ 3a, 7″, 6C (5C+1), 6S, 5‴, 2⁗. Plate 1a and 3a adjacent, hexagonal and similar in shape. Plate 2a below and between plates 1a and 3a, subrectangular to rounded in shape. Sulcus well defined, not extending to the antapex. Anterior sulcal plate (S_a) broader than long, extending over flagella pore and sulcal plates. Nucleus large, spherical and positioned in the hypotheca. Cells contain several globular, peripherally placed, dark brown-green chloroplasts. Resting cysts spherical to ovoid, 20–26 μm diameter, with numerous nontabular calcareous acicular or capitate spines of 3.5–4.5 μm in length.

HOLOTYPE: Figure 2; Strain SCBC17; established from an individual resting cyst germinated and cultured from coastal sediments collected from Bahoo-Kalat estuary, southeast coast of Iran, March 2004. Cultures are maintained at the University of Tasmania, School of Aquaculture, Algae Culture Unit, Launceston, Australia.

TYPE LOCALITY: Bahoo-Kalat Estuary, Iran.

ETYMOLOGY: '*irregularis*' — in which symmetry is destroyed by some inequality of parts; referring to the lack of symmetry of the anterior intercalary plates.

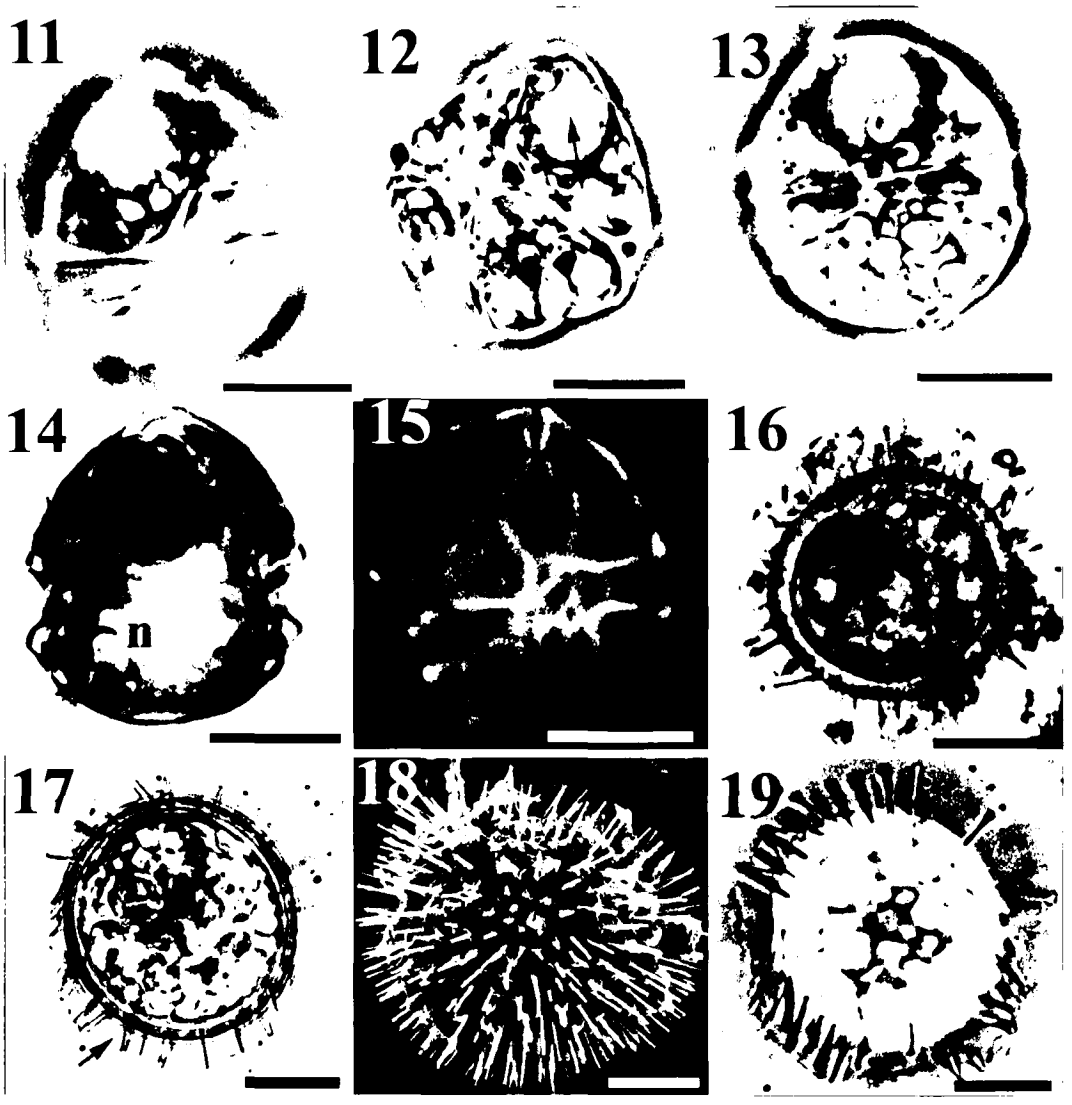

Figs 11–19. Light microscopy. Vegetative cells and cysts of *Scrippsiella irregularis*. All scale bars = 10 μm.
Fig. 11. Ventral view of cell showing cingulum displacement.
Fig. 12. Ventrolateral view. Arrow showing large accumulation body.
Fig. 13. Dorsal view showing the cingulum narrowing on dorsal side (arrow).
Fig. 14. Dorsal view of cell showing the large nucleus (n) in the hypotheca. Note irregular arrangement and shape of the chloroplasts (arrow).
Fig. 15. Calcofluor-stained cell showing the ventral plate patterns.
Fig. 16. Light microscopy. Resting cyst isolated from sediment.
Fig. 17. Light microscopy. Cultured resting cyst showing cell content and accumulation body. Note the transparent membrane surrounding the spines (arrow).
Fig. 18. SEM. Wild cyst showing the calcareous spines.
Fig. 19. Light microscopy. Cultured cyst with surface focus showing the spines.

DISTRIBUTION: Southern coast of Iran, Bahoo-Kalat Estuary.

REMARKS: The vegetative cells of cultures SCBC17 and SCBC19 are ovoid and slightly dorsoventrally compressed and possess a rounded epitheca with convex sides. The apex is rounded with no pronounced apical horn (Figs 2–5). The hypotheca is semicircular in outline. The cells are 17–29 μm ($\bar{X}$ = 22 μm, n = 50) in length and 13-23μm ($\bar{X}$ = 18 μm, n = 50) in width. The epitheca is longer than the hypotheca (length : width ratio = 1.4). The cingulum is left-handed and displaced one-half to one cingulum width (Figs 2, 5, 11). The cingular width varies from 2.6 to 3.6 μm ($\bar{X}$ = 2.9 μm, n = 20). The border between the cingulum and hypotheca is curved, and the cingulum narrows slightly on the dorsal side (Figs 3, 13). The dorsal narrowing can be observed in both fixed and live cells by light microscopy and SEM; however, this may be accentuated by slight cell compression under a coverslip or cell swelling during SEM fixation. The plate formula is the same as other *Scrippsiella* species [i.e. Po, X, 4', 3a, 7'', 6C (5C+1 transitional plate = T-plate), 5S, 5''', 2''''; see Figs 2, 4, 5, 7], but the shape, position, and relationship between the three anterior

intercalary plates is atypical. The plates are located diagonally on the dorsal part of the epicone (Figs 3, 4); plates 1a and 3a are six-sided and in contact on their anterior margins (Fig. 4). Plate 2a is subrectangular with two convex sides and is positioned between the posterior margins of plates 1a and 3a (Figs 3, 4, 10).

The sulcus is composed of five plates: S_a, S_p, S_s, S_d, and S_m plates (Figs 2, 5). S_a is located between 1′ and 7″ and exhibits a hook-like extension over the flagellar pore, the sulcal plates, and the border with the T-plate (Figs 5, 15). The S_p plate contacts the T-plate and extends into the hypotheca without reaching the antapex (Fig. 5). The S_s plate is small and rhomboidal in shape and connected to the T-plate on the left side (Figs 2, 9). The S_d plate is triangular and positioned beneath the S_a plate, touching the 7″, 6C, 5‴, and S_p plates (Figs 5, 6). The S_m plate is almost completely hidden by the anterior part (wing) of the S_p plate (Fig. 5) and can be seen when the S_d plate is damaged (Fig. 9). The first cingulum plate (T-plate) is notched on the right margin where it meets the borders of the S_s plates and also contacts the S_a plate (Figs 9, 15).

Cells contain several peripherally placed brown-green chloroplasts that are round to oval in shape and irregularly arranged (Figs 13, 14). The spherical nucleus is prominent as a pale region positioned in the hypotheca (Fig. 14), and a large yellowish-orange accumulation body is visible in the epitheca near the apex of cultured cells (Figs 11–14). Laboratory cultured cells show positive growth at temperatures ranging from 17°C to 27°C. Resting cysts were produced when cultures were grown in nitrate- and phosphate-deficient media; however, cyst concentrations were usually low and were not significantly altered over the 17–27°C temperature range investigated here. No encystment was noted in nutrient-replete cultures.

Cultured resting cysts are covered with numerous, narrow, slightly tapered nontabular calcareous spines. A clear thin outer membrane is often evident surrounding the spines produced in culture (Figs 17, 19). Similar calcareous cysts were also isolated from the sediment samples (Figs 16, 18). However, both *S. irregularis* cultures were germinated from a clear-walled, spineless cyst. Cultured cysts are spherical to oval in shape and grey-brown in colour with a prominent red-orange accumulation body. Cyst body diameter ranges from 20 to 26 μm ($\bar{X}$ = 24 μm, n = 15) in diameter, with the process length ranging from 3.5 to 4.5 μm (average = 4 μm, n = 15). Cultured cysts have both capitate and pointed spines, whereas wild cysts appeared to have only pointed spines. No clearly defined archeopyle was observed in germinated specimens.

Phylogenetic analyses

Significant negative skewness of the random tree distribution was observed in both the NJ analysis including 56 taxa ($g1 = -0.511$, $P < 0.01$) and the MP analysis including 27 taxa ($g1 = -0.915$, $P < 0.01$), indicating that the data sets were phylogenetically informative. Both analyses produced trees with similar branching of major clusters; therefore, only the MP analysis with 27 taxa is shown (Fig. 20). The Calciodinelloidean taxa formed two major clades: the *Ensiculifera* Balech species and *Pentapharsodinium dalei* Indelicate & Loeblich form a well-supported cluster (92% bootstrap support); the remaining *Scrippsiella*-like species (SCR clade) form a second major cluster with moderate (74%) boostrap support. *Scrippsiella hangoei* Schiller consistently occupied a basal position among the *Scrippsiella* species in the analyses. The SCR clade includes members of the genera *Scrippsiella*, *Calciodinellum* Deflandre, *Calcigonellum* Deflandre, and *Pernambugia* Janofske & Karwath. Within the SCR clade, three clusters are evident, referred to here as SCR.A, SCR.B, and SCR.C (Fig. 20). Both strains of *S. irregularis* cluster with *Scrippsiella precaria* and *S. ramonii* with 100% bootstrap support (SCR.A). The new species *S. irregularis* is most closely related to *S. precaria* (15.5% sequence divergence) and then *S. ramonii* (17% sequence divergence). The second cluster (SCR.B) includes the *Scrippsiella trochoidea* complex, *Calciodinellum levantinum* Meier, Janofske & Willems, and *Scrippsiella trifida* Lewis. The third cluster (SRC.C) includes *Calciodinellum albatrosianum*, *C. operosum*, *Calciodinellum* sp., with *Scrippsiella infula* and *Scrippsiella rotunda* forming a related sister group to the *Calciodinellum* species. Three species, *S. sweeneyae* (Balech) Loeblich, *S. lachrymosa* Lewis, and *Pernambugia tuberosa* Kamptner & Janofske, are not clearly allied with any of the three clusters.

DISCUSSION

The primary taxonomic feature for separating *Scrippsiella* species is the arrangement and shape of the thecal plates (Fensome *et al.* 1993; D'Onofrio *et al.* 1999; Montresor *et al.* 1997; Janofske 2000). The typical plate pattern in the genus is Po, X, 4′, 3a, 7″, 6C (5C+ 1 T-plate), 5S, 5‴ and 2⁗. In most species the anterior intercalary plates are symmetrically arranged, with pentagonal 1a and 3a plates separated by a hexagonal 2a plate. However, plate tabulation within the genus is highly conserved; therefore, cell shape and outline and the shape of various thecal plates are considered important features separating species (Montresor *et al.* 2003).

The anterior dorsal plate pattern of *S. irregularis* differs from the more typical symmetrical arrangement. The 1a and 3a plates are asymmetrically arranged and in direct contact with each other, and the 2a plate contacts both the 1a and 3a plates on the posterior margin. This asymmetrical arrangement of the dorsal epithecal plates is known as cinctioid tabulation (Fensome et al. 1993) and matches the cinctioid tabulation (*sensu* Fensome *et al.* 1993) of both *S. precaria* (Montresor & Zingone 1988) and *S. ramonii* (Montresor 1995).

The general cell morphology and tabulation of *S. irregularis* is more similar to *S. precaria* than *S. ramonii*, the latter readily distinguished by a prominent antapical horn on the 2⁗ plate (Montresor 1995). The cell shape of *S. irregularis* is more rounded than *S. precaria* (Fig. 21), but its dome-shaped epitheca is more similar to that of *S. ramonii*. Despite the similarities in plate patterns of all three cinctioid *Scrippsiella* species, the shape and relative size of some plates and cytological features are sufficiently different to distinguish *S. irregularis*. Firstly, the subrectan-

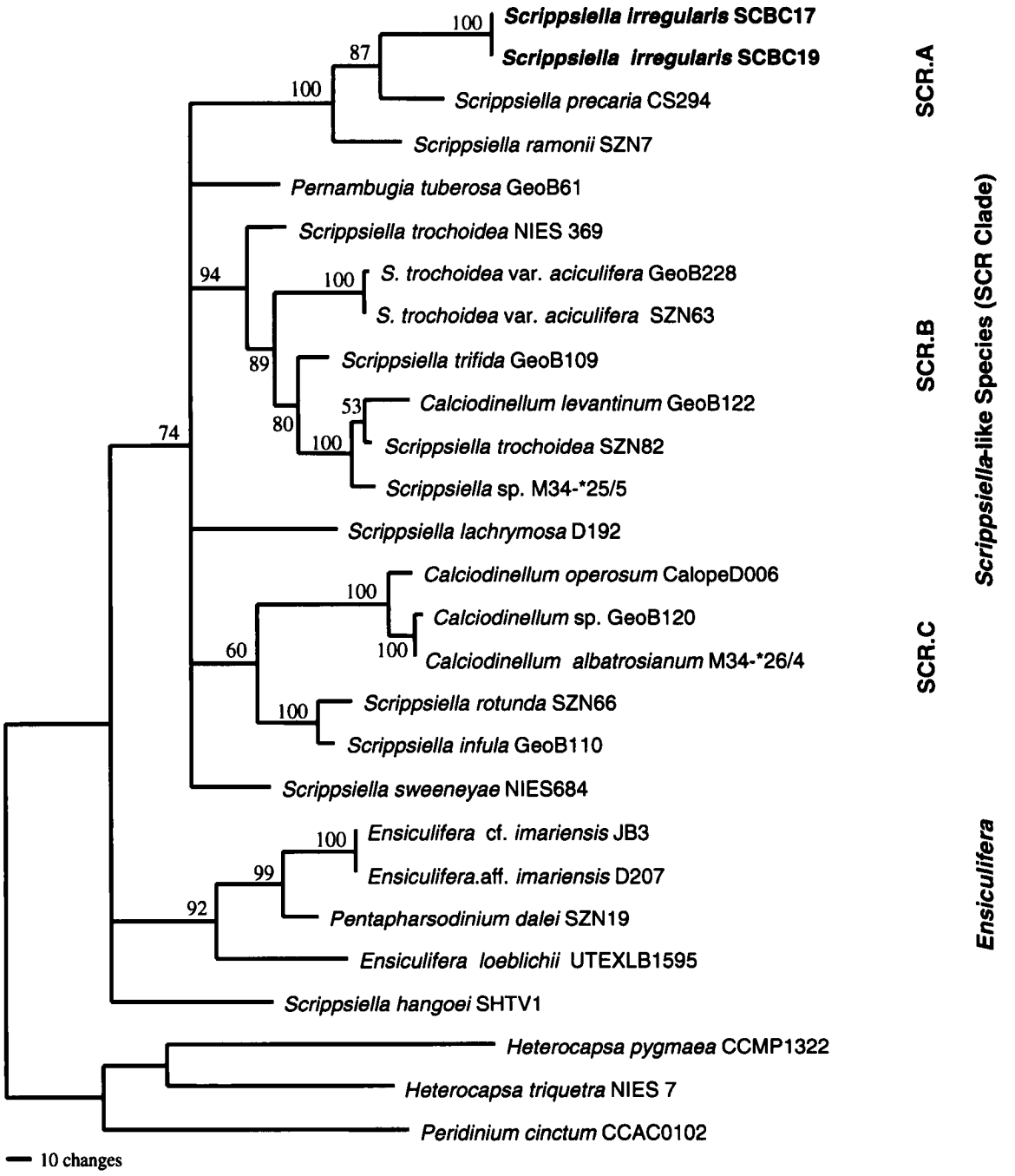

Fig. 20. Phylogeny of 27 taxa of Calciodinellaceae inferred from 5.8s and both ITS1 and ITS2 of rRNA region. A bootstrap consensus tree obtained by parsimony analysis from 100 replicates using the branch and bound search option of PAUP 4.0*. Bootstrap support for each cluster is indicated; branches with <50% support are collapsed to polytomies. *Heterocapsa triquetra*, *H. pygmaea*, and *Peridinium cinctum* were used as outgroup taxa. Species from the present study are indicated in bold. The three subclades SCR.A, SCR.B, and SCR.C within the genus *Scrippsiella* (Gottschling *et al.* 2005) and the genus *Ensiculifera* are indicated by the shaded boxes.

gular 2a plate of *S. irregularis* is much larger than the small diamond-shaped 2a plate of *S. precaria* and more similar to the 2a plate of *S. ramonii*, which possesses two curved sides. Secondly, the narrower cingulum of *S. irregularis* is also clearly more equatorially placed than the cingulum of *S. precaria* (Fig. 21). Thirdly, the shape and conformation of the sulcal plates of *S. irregularis* differ from *S. precaria*. The transitional plate of *S. irregularis* terminates at the junction of the 1′ and 1″ plates, and the first apical plate as in *S. precaria* (compare fig. 1a from Montresor & Zingone 1988) extends apically to border the 1′ plate, although it is possible that this connection may vary within *S. precaria*. Finally, the nucleus is located in the hypotheca, whereas the nucleus of *S. precaria* is in the anterior part of the cell, almost entirely above the equatorial plane (Montresor & Zingone 1988).

The cysts of *S. precaria* and *S. irregularis* are very similar. Both are spherical to subspherical and covered with

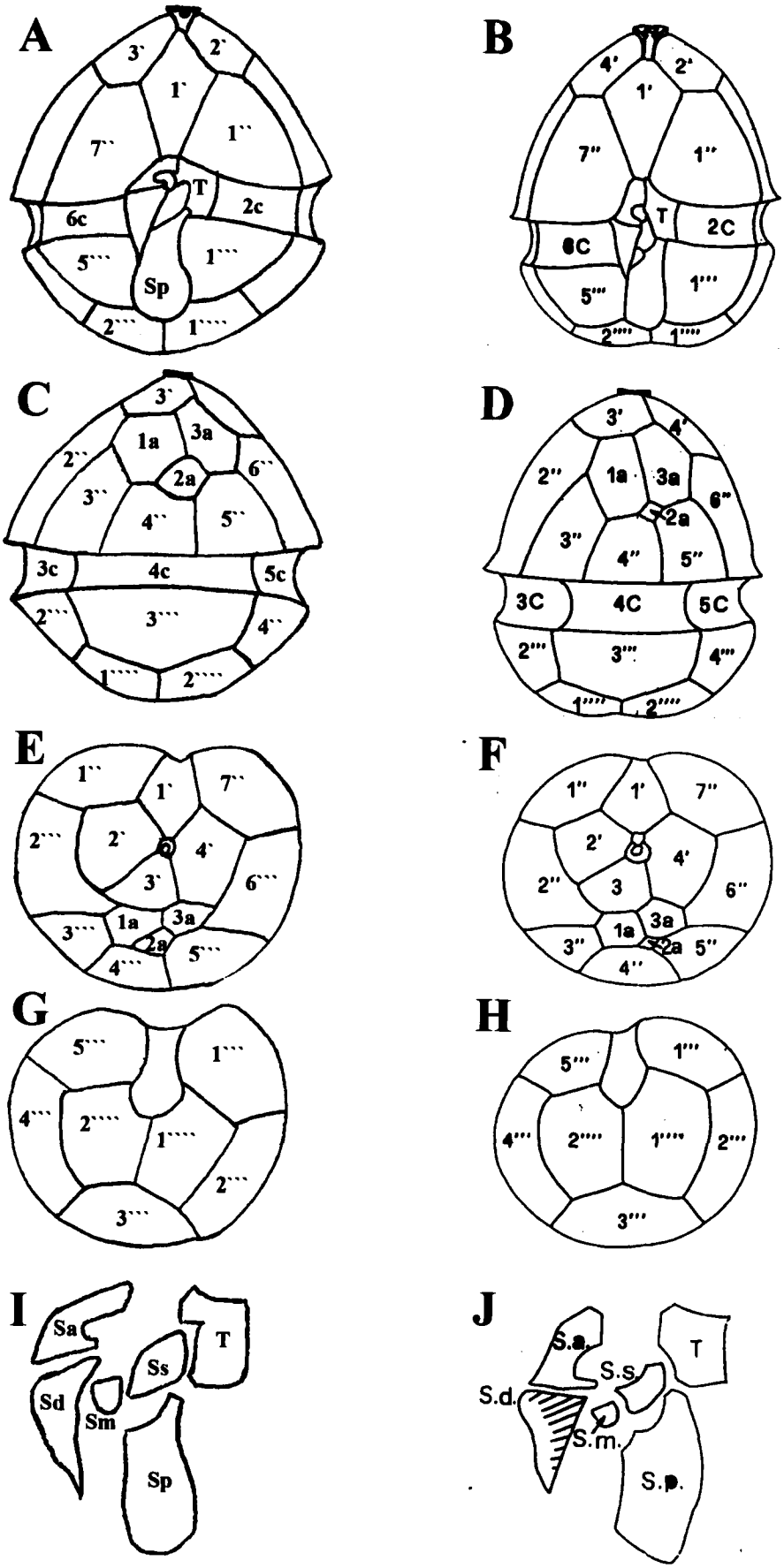

Table 2. Morphological comparison of motile cells and resting cysts of *Scrippsiella irregularis* sp. nov., *Scrippsiella precaria* (Montresor & Zingone 1988), and *Scrippsiella ramonii* (Montresor 1995).

Feature	*S. ramonii*	*S. precaria*	*S. irregularis*
Motile cells			
Length (μm)	22–34	15–25 ($\bar{X}$ = 19.2)	17–29 ($\bar{X}$ = 22)
Width (μm)	19–27	13.8–20 ($\bar{X}$ = 16)	13–23 ($\bar{X}$ = 18)
Cingulum width (μm)	?	($\bar{X}$ = 4.1)	2.6–3.6 ($\bar{X}$ = 2.9)
Cingulum displacement	?	2/3 of its width	1/2–1 of its width
Cell apex	rounded	rounded	rounded
Cell antapex	small horn	flattened	rounded
Epitheca/hypotheca ratio	? longer	1.6	1.4
2a plate; size shape	large rhombic	small rhomboidal	medium rounded subrectangular
Nucleus; shape	spherical	spherical	spherical
Position	central	anterior	posterior
Colour	yellow-green	olive-green	brown-green
Resting cysts			
Size (μm)	31–36 long 25–26 wide	17.5–25 ($\bar{X}$ = 20.5); 15–23 ($\bar{X}$ = 18.6)	20–26 ($\bar{X}$ = 24)
Cyst shape	ovoid	spherical to oval	spherical to subspherical
Colour	dark brown	light brown	light brown-grey
Process termination	capitate	generally pointed, sometimes capitate	pointed and capitate spines
Process length (μm)	9–11.5	3.1–6.9 ($\bar{X}$ = 4.7)	3.6–4.5 ($\bar{X}$ = 4)

nontabular calcareous spines; however, *S. irregularis* cysts are slightly larger with slightly shorter spines (Table 1). Cysts of *S. ramonii* are somewhat more easily distinguished by their oval shape, dark brown colour, and significantly longer calcareous processes (Montresor 1995).

The phylogenetic analysis presented here identifies three main clusters within *Scrippsiella* that have been identified by previous studies (D'Onofrio *et al.* 1999; Montresor *et al.* 2003; Gottschling *et al.* 2005). While each cluster is composed of morphologically similar strains, there is no clear link between the clustering and cell or cyst morphology of the species within each cluster. The exception is the cluster of species (SCR.A) that includes *S. precaria*, *S. ramonii*, and *S. irregularis* sp. nov. All three possess the distinctive asymmetrical arrangement of intercalary plates (Montresor & Zingone 1988; Montresor 1995) and have a wide rhomboidal first apical plate. Asymmetrically arranged anterior intercalary plates are also a feature of *S. hangoei* Schiller, yet our phylogenetic analyses indicate that *S. hangoei* is distinct from the SCR.A cluster and other *Scrippsiella* species. In this species, plates 1a and 2a are irregularly pentagonal rather than hexagonal, and plate 3a is much larger and hexagonal rather than rhomboidal. Resting cysts of *S. hangoei* differ from other *Scrippsiella* species by having an organic wall bearing furcate organic processes rather than calcareous spines (Larsen *et al.* 1995). Cultured resting cysts are spherical and smooth-walled and lack furcate processes (Kremp *et al.* 2005). Three benthic *Scrippsiella*-like species recently transferred to the genus *Bysmatrum* Faust & Steidinger also show asymmetrical anterior intercalary tabulation, but, in this genus, plates 2a and 3a are separated by the 3′ plate, and the thecal plates have a reticulated surface (Faust & Steidinger 1998). All other *Scrippsiella* species generally exhibit a symmetrical anterior intercalary plate arrangement composed of a hexagonal 2a plate inserted between pentagonal 1a and 3a plates.

The highly supported clustering of *S. irregularis* sp. nov. with *S. precaria* and *S. ramonii* in our phylogenetic analyses (SCR.A) strongly supports our placement of the new species within *Scrippsiella* as part of the group possessing cinctioid epithecal tabulation. While *S. irregularis* is morphologically similar to *S. precaria*, the sequence divergence between these two species is greater than that between *S. precaria* and *S. ramonii*. Combined with the morphological differences, our data clearly support our recognition of *S. irregularis* as a new species distinct from *S. precaria* and *S. ramonii*.

ACKNOWLEDGEMENTS

The authors thank Sharareh Khodami from the Iranian Fisheries Research Institute (IFRI) for sediment collection and arranging sample transport to Australia. We also thank Geraldine Nash (Antarctic Division, Hobart, Australia), Dr Tae-Gyu Park (School of Plant Science, University of Tasmania, Hobart, Australia), and David Steele (Central Science Laboratory, University of Tasmania, Hobart, Australia) for assistance with SEM preparation and imaging.

←

Fig. 21. Schematic drawing of the thecal plates of *Scrippsiella irregularis* (left column) compared with the thecal plates of *Scrippsiella precaria* (right column) (from Montresor & Zingone 1988). A, B: ventral view; C, D: dorsal view; E, F: apical view; G, H: antapical view; and I, J: sulcal plates.

REFERENCES

ADACHI M., SAKO Y. & ISHIDA Y. 1994. Restriction fragment length polymorphism of ribosomal DNA internal transcribed spacer and 5.8s-regions in Japanese *Alexandrium* species (Dinophyceae). *Journal of Phycology* 30: 857–863.

BLACKBURN S.I., HALLEGRAEFF G.M. & BOLCH C.J. 1989. Vegetative reproduction and sexual life-cycle of the toxic dinoflagellate *Gymnodinium catenatum* from Tasmania, Australia. *Journal of Phycology* 25: 577–590.

BOLCH C.J.S. 1997. The use of sodium polytungstate for the separation and concentration of living dinoflagellate cysts from marine sediments. *Phycologia* 36: 472–478.

BOLCH C.J. & HALLEGRAEFF G.M. 1990. Dinoflagellate cysts in recent marine sediments from Tasmania, Australia. *Botanica Marina* 33: 173–192.

BOLCH C.J., BLACKBURN S.I., HALLEGRAEFF G.M. & VAILLANCOURT R.E. 1998. Genetic variation among different global populations of *Gymnodinium catenatum* revealed by RAPD-PCR. In: *Harmful microalgae* (Ed. B. Reguera, J. Blanco, M.L. Fernandez & T. Wyatt), pp. 283–286. Xunta de Galicia and UNESCO, Paris.

DALE B. 1992. Dinoflagellate contributions to the open ocean sediment flux. In: *Dinoflagellate contributions to the deep sea* (Ed. B. Dale & A.L. Dale), pp. 1–31. Woods Hole Oceanographic Institution Ocean Biocoenosis Series, Woods Hole, Massachusetts.

D'ONOFRIO G., MARINO D., BIANCO L., BUSICO E. & MONTRESOR M. 1999. Toward an assessment on the taxonomy of dinoflagellates that produce calcareous cysts (Calciodinelloideae, Dinophyceae): a morphological and molecular approach. *Journal of Phycology* 35: 1063–1078.

FAUST M.A. 1996. Morphology and ecology of the marine benthic dinoflagellate *Scrippsiella subsalsa* (Dinophyceae). *Journal of Phycology* 32: 669–675.

FAUST M.A. & STEIDINGER K.A. 1998. *Bysmatrum* gen. nov. (Dinophyceae) and three new combinations for benthic scrippsielloid species. *Phycologia* 37: 47–52.

FELSENSTEIN J. 1985. Confidence limits on phylogenies: an approach using the bootstrap. *Evolution* 39: 783–791.

FENSOME R.A., TAYLOR F.J.R., NORRIS G., SARGEANT W.A.S., WHARTON D.I. & WILLIAMS L.G. 1993. *Classification of living and fossil dinoflagellates* American Museum of Natural History, New York, 351 pp.

FRITZ L. & TREIMER R.E. 1985. A rapid simple technique utilizing calcofluor white M2R for the visualization of dinoflagellate thecal plates. *Journal of Phycology* 21: 662–664.

GODHE A., KARUNASAGAR I. & KARLSON B. 2000. Dinoflagellate cysts in recent marine sediments from SW India. *Botanica Marina* 43: 39–48.

GOTTSCHLING M., KNOP R., PLOTNER J., KIRSCH M., WILLEMS H. & KEUPP H. 2005. A molecular phylogeny of Scrippsiella *sensu lato* (Calciodinellaceae, Dinophyta) with interpretations on morphology and distribution. *European Journal of Phycology* 40: 207–220.

HALL T.A. 1999. BioEdit: a user-friendly biological sequence alignment editor and analysis program for Windows 95/98/NT. *Nucleic Acids Research, Symposium Series* 41: 95–98.

HILLIS D.M. & HUELSENBECK J.P. 1992. Signal, noise, and reliability in molecular phylogenetic analyses. *Journal of Heredity* 83: 189–195.

HONSELL G. & CABRINI M. 1991. *Scrippsiella spinifera* sp. nov. (Pyrrhophyta): a new dinoflagellate from the northern Adriatic Sea. *Botanica Marina* 34: 167–175.

JANOFSKE D. 2000. *Scrippsiella trochoidea* and *Scrippsiella regalis*, nov. comb. (Peridiniales Dinophyceae): a comparison. *Journal of Phycology* 36: 178–189.

JEANMOUGIN F., THOMPSON J.D., GOUY M., HIGGINS D.G. & GIBSON T.J. 1998. Multiple sequence alignment with Clustal X. *Trends in Biochemical Sciences* 23: 403–500.

KOBAYASHI S. & MATSUOKA K. 1995. A new species of *Ensiculifera*, *E. imariense* (Dinophyceae), producing organic-walled cysts. *Journal of Phycology* 31: 147–152.

KREMP A., ELBRÄCHTER M., SCHWEIKERT M., WOLNY J.L. & GOTTSCHLING M. 2005. *Woloszynskia halophyla* (Biecheler) comb. nov.: a bloom-forming cold-water dinoflagellate co-occurring with *Scrippsiella hangoei* (Dinophyceae) in the Baltic Sea. *Journal of Phycology* 41: 629–643.

LARSEN J., KUOSA H., IKAVALKO J., KIVI K. & HALLFORS S. 1995. A redescription of *Scrippsiella hangoei* (Schiller) comb. nov., a red tide dinoflagellate from the northern Baltic. *Phycologia* 34: 135–144.

MARCHANT H. & THOMAS D. 1983. Polylysine as an adhesive for the attachment of nanoplankton to substrates for electron microscopy. *Journal of Microscopy* 131(1): 127–129.

MONTRESOR M. 1995. *Scrippsiella ramonii* sp. nov. (Peridiniales, Dinophyceae), a marine dinoflagellate producing a calcareous resting cyst. *Phycologia* 34: 87–91.

MONTRESOR M. & ZINGONE A. 1988. *Scrippsiella precaria* sp. nov. (Dinophyceae), a marine dinoflagellate from the Gulf of Naples. *Phycologia* 27: 387–394.

MONTRESOR M., JANOFSKE D. & WILLEMS H. 1997. The cyst-theca relationship in *Calciodinellum operosum* emend. (Peridiniales, Dinophyceae) and a new approach for the study of calcareous cysts. *Journal of Phycology* 33: 122–131.

MONTRESOR M., SGROSSO S., PROCACCINI G. & KOOISTRA W. 2003. Intraspecific diversity in *Scrippsiella trochoidea* (Dinophyceae): evidence for cryptic species. *Phycologia* 42: 56–70.

NATION J.L. 1983. A new method using hexamethyldisilazane for preparation of soft insect tissues for scanning electron microscopy. *Stain Technology* 58: 347–351.

SWOFFORD D.L. 2002. PAUP*: *phylogenetic analysis using parsimony and other methods.* Version 4. Sinauer Associates, Sunderland, Massachusetts.

VINK A. 2004. Calcareous dinoflagellate cysts in south and equatorial Atlantic surface sediments: diversity, distribution, ecology and potential for palaeoenvironmental reconstruction. *Marine Micropaleontology* 50: 43–88.

Received 2 January 2007; accepted 14 May 2007
Associate editor: Stuart Sym